

Roles of Fission Yeast Grc3 Protein in Ribosomal RNA Processing and Heterochromatic Gene Silencing^{*[S]}

Received for publication, November 7, 2010, and in revised form, March 1, 2011. Published, JBC Papers in Press, March 8, 2011, DOI 10.1074/jbc.M110.201343

Erina Kitano^{‡S1}, Aki Hayashi[‡], Daigo Kanai^{¶1}, Kaori Shinmyozu^{||}, and Jun-ichi Nakayama^{‡¶12}

From the [‡]Laboratory for Chromatin Dynamics and ^{||}Proteomics Support Unit, RIKEN Center for Developmental Biology, Kobe Hyogo 650-0047, Japan, the ^SDepartment of Biology, Graduate School of Science, Kobe University, Kobe 657-8501, Japan, and the [¶]Department of Bioscience, Graduate School of Science and Technology, Kwansai-Gakuin University, Sanda 669-1337, Japan

Grc3 is an evolutionarily conserved protein. Genome-wide budding yeast studies suggest that Grc3 is involved in rRNA processing. In the fission yeast *Schizosaccharomyces pombe*, Grc3 was identified as a factor exhibiting distinct nuclear dot localization, yet its exact physiological function remains unknown. Here, we show that *S. pombe* Grc3 is required for both rRNA processing and heterochromatic gene silencing. Cytological analysis revealed that Grc3 nuclear dots correspond to heterochromatic regions and that some Grc3 is also present in the nucleolar peripheral region. Depleting the heterochromatic proteins Swi6 or Clr4 abolished heterochromatic localization of Grc3 and resulted in its preferential accumulation in the perinucleolar region, suggesting its dynamic association with these nuclear compartments. Cells expressing mutant *grc3* showed defects in 25 S rRNA maturation and in heterochromatic gene silencing. Protein analysis of Grc3-containing complexes led to the identification of Las1 and components of the IPI complex (Rix1, Ipi1, and Crb3). All of these Grc3-interacting proteins showed a dynamic nuclear localization similar to that observed for Grc3, and those conditional mutants showed defects in both rRNA processing and silencing of centromeric transcripts. Our data suggest that Grc3 functions cooperatively with Las1 and the IPI complex in both ribosome biogenesis and heterochromatin assembly.

Although the eukaryotic nucleus appears relatively unstructured compared with the cytoplasm, it contains a variety of functional compartments (1). The nucleolus, the most striking example of a functional nuclear compartment, is important in ribosome biogenesis (2). High level organization related to nuclear function also exists in the extranucleolar nucleoplasm. For example, heterochromatin, a densely packed nuclear subdomain, is a type of nuclear compartment with essential roles in nuclear organization and chromosome structure (3). Although these two nuclear compartments are distinct, there is increas-

ing evidence that they use similar molecular mechanisms for epigenetic gene regulation (2, 4).

In the fission yeast *Schizosaccharomyces pombe*, heterochromatin domains are found at telomeres, the silent mating type locus, and on pericentromeric repeats. Heterochromatin establishment correlates with changes in post-translational histone tail modification. Clr4, a mammalian SUV39H homologue, provides histone H3 lysine 9 methylation (H3K9me)³ on heterochromatin, which then serves as a docking site for the HP1 proteins Swi6 and Chp2 (5–8). In most eukaryotes, HP1/Swi6 and H3K9me play a critical role in maintaining higher order chromatin structure and ensuring faithful chromosome segregation (9).

Although heterochromatin has long been thought to be transcriptionally silent, recent studies have shown that it is transcriptionally active and that the processing of transcribed RNAs is tightly coupled with heterochromatin formation. For example, heterochromatin assembly at fission yeast centromeres requires components of the RNAi pathway (10–12). Centromeric *dg* and *dh* repeats are transcribed by RNA polymerase II, and the processing of nascent transcripts through the RNAi pathway is coupled with the H3K9me introduction and heterochromatin spreading (13). A second RNA processing pathway, involving Cid14 poly(A) polymerase and the exosome, is required for efficient heterochromatic gene silencing (14, 15). Therefore, it is likely that heterochromatic transcripts are targeted and degraded by the exosome and/or RNAi machinery, with the help of other RNA processing machineries.

Transcribed RNA processing also plays a central role in nucleolar function. In all organisms, the synthesis of ribosomal RNAs (5, 5.8, 18, and 25–28 S rRNA) is not achieved by simply transcribing the individual rRNA species but requires a complex series of post-transcriptional processing steps. Three of the four rRNAs (18, 5.8, and 25 S) are transcribed by RNA polymerase I as a single large precursor, 35 S pre-rRNA, that contains the sequences for mature 18, 5.8, and 25 S rRNAs, along with two external transcribed spacers and two internal transcribed spacers (ITS1 and ITS2). During the maturation process, the pre-rRNA has to undergo a number of modifications and is subjected to cleavages and trimming events. Studies on *Saccharomyces cerevisiae* have revealed that a remarkable number of trans-acting factors, including small nucleolar

* This work was supported by a grant-in-aid from the Ministry of Education, Culture, Sports, Science, and Technology of Japan.

[S] The on-line version of this article (available at <http://www.jbc.org>) contains supplemental Tables S1–S3 and Figs. S1–S3.

¹ Supported by the Global Center of Excellence (G-COE) program of Kobe University.

² To whom correspondence should be addressed: RIKEN Center for Developmental Biology, 2-2-3 Minatojima-minamimachi, Chuo-ku, Kobe Hyogo 650-0047, Japan. Tel.: 81-78-306-3205; Fax: 81-78-306-3208; E-mail: jnakayama@cdb.riken.jp.

³ The abbreviations used are: H3K9me, H3 lysine 9 methylation; ITS, internal transcribed spacer.

Analysis of *Grc3* Function in *S. pombe*

RNAs, small nucleolar RNP proteins, putative RNA helicases, endo- and exoribonucleases, and putative ATP/GTPases, are involved in rRNA maturation and assembly into ribosomal subunits (16, 17). Although recent genome-wide approaches have uncovered a number of additional factors that are potentially involved in rRNA processing (18, 19), their detailed roles in rRNA and ribosome processing remain unresolved.

Grc3 is a widely conserved eukaryotic protein that possesses a conserved ATP/GTPase domain and shows extensive sequence similarity to Clp1, a component of the mRNA cleavage and polyadenylation machinery (20, 21). In *S. cerevisiae*, Grc3 is essential for growth (22), and genome-wide studies have shown that it is involved in rRNA processing, especially in the ITS2 processing (18). In *S. pombe*, however, the Grc3 homologue encoded by *SPCC830.03* was identified in genome-wide localization screenings as a factor displaying “nuclear dot” localization (23–25). Although heterochromatin shares this characteristic nuclear dot localization pattern in fission yeast (6, 26), functional involvement of Grc3 with heterochromatin or rRNA processing remains unknown.

In this study, we show that fission yeast Grc3 dynamically associates with both heterochromatic and perinucleolar regions and is required for both rRNA processing and heterochromatic gene silencing. We further demonstrated that Grc3 is functionally linked with the IPI complex and Las1. The processing of transcribed RNA is critical to both ribosome assembly and heterochromatic gene silencing, and this study reveals that a common mechanism involving Grc3 underlies these distinct nuclear processes.

EXPERIMENTAL PROCEDURES

Strains and Plasmids—The *S. pombe* strains used in this study are listed in supplemental Table S1. Tagging to produce GFP and FLAG fusion proteins of endogenous *grc3*⁺, *crb3*⁺, *las1*⁺, *rix1*⁺, and *ipi1*⁺ was performed using a PCR-based gene targeting protocol (27). Endogenous *clr4*⁺ and *swi6*⁺ were deleted by a PCR-based method or by standard genetic crosses. To express wild-type or mutant Grc3 from a multicopy plasmid, the Grc3 coding sequence was first cloned into pREP1 plasmid, and mutation was introduced by *in vitro* mutagenesis method as described previously (6).

Microscopy Analysis—Immunofluorescence experiments were performed as described previously (6). Wild-type and mutant *S. pombe* cells expressing each of the GFP fusion proteins were cultured on minimal medium. Single colonies were picked and patched onto new plates. The cells were grown to early log phase in liquid medium and washed twice with deionized H₂O, and the DNA was visualized by incubation with 1 μg/ml Hoechst 33342. Microscopic images were obtained on a Zeiss Axioplan2 imaging microscope and an ORCA-ER camera (Hamamatsu) or an Olympus IX71-based three-dimensional microscope system and a CoolSNAP HQ (Photometrics). Three-dimensional optical section images were taken at six focal planes with 0.5-μm focus intervals using MetaMorph (Universal Imaging), and the acquired images were deconvoluted and analyzed by softWoRX (Applied Precision).

ChIP—ChIP was performed as described previously (6). Anti-FLAG M2 affinity gel (Sigma) was used to immunopre-

cipitate FLAG-tagged proteins. The anti-Swi6 polyclonal antibody was described previously (6). PCR products were separated and analyzed by electrophoresis on a 15% polyacrylamide gel. Primers used in this assay are listed in supplemental Table S2.

Protein Affinity Purification—Grc3-TAP, Las1-TAP, and Crb3-TAP purifications were done as described previously (28), with some modifications. The cells were grown in YEA medium (0.5% yeast extract, 3% glucose, 75 μg/ml adenine) to an *A*₅₉₅ of 2–3. The cells were spun at 4 °C and washed once with STOP buffer (150 mM NaCl, 50 mM NaF, 10 mM EDTA, 1 mM NaN₃, pH 8.0). The cell pellet (1 × 10¹⁰ cells in a 50-ml Falcon tube) was resuspended in 0.5 ml of Nonidet P-40 lysis buffer (50 mM HEPES/NaOH, pH 7.9, 150 mM NaCl, 1 mM EDTA, 1% Nonidet P-40, 0.1 mM Na₃VO₄, 1 mM DTT, 1 mM PMSF), supplemented with protease inhibitor mixture (Complete; Roche Applied Science), and lysed by vortexing with zirconia beads (for 2 min five times at 4 °C, with 2-min intervals on ice). The crude cell lysate was diluted with 10 ml of Nonidet P-40 lysis buffer and incubated with gentle agitation on a disc rotator for 15 min at 4 °C. The extract was spun at 12,000 × *g* for 10 min at 4 °C. Lysates were then transferred to a 50-ml Falcon tube and incubated with 400 μl of prewashed IgG-Sepharose 6 Fast Flow (GE Healthcare) for 2–3 h at 4 °C. The beads and immobilized proteins were harvested by centrifugation at 400 *g*, loaded on a Bio-Rad Poly-Prep column, and washed three times with 10 ml of Nonidet P-40 lysis buffer. Bound protein was eluted with 1 ml of tobacco etch virus protease cleavage buffer containing 50–100 units of AcTEVTM Protease (Invitrogen) at 4 °C overnight. The elute was then incubated with 200 μl of calmodulin affinity resin (Stratagene), and the bound protein was eluted as described previously (28). Eluted proteins were precipitated by adding 2 volumes of ethanol, resolved by SDS-PAGE, and subjected to LC-MS/MS analysis.

Mass Spectrometry—Affinity-purified proteins were resolved by 4–20% SDS-PAGE (Daiichi). After silver staining, the peptide bands were excised from the gel and subjected to in-gel reduction with 10 mM DTT, alkylation with 55 mM iodoacetamide, and digestion with 10 μg/ml modified Trypsin (Promega) at 37 °C for 16 h. After in-gel digestion, the collected phosphorylated peptides were subjected to mass spectrometry analysis as described previously (29).

Isolation of Temperature-sensitive Mutants—The *grc3*⁺ genomic region (from 80 bp upstream of ATG to 650 bp downstream of the stop codon) was first PCR-amplified using KOD polymerase (Toyobo) and cloned into the pCRII-TOPO vector (Invitrogen). After sequencing, the 1.8-kb *ura4*⁺ reporter gene was introduced downstream of the *grc3*⁺ coding region (ClaI site, 287 bp downstream of the stop codon). To isolate temperature-sensitive mutants for *crb3*⁺, *ipi1*⁺, *las1*⁺, or *rix1*⁺, a downstream part of each coding region (~1 kb) and a 3'-untranslated region (300–500 bp) were first amplified using KOD polymerase (Toyobo), and these PCR products were then used for second PCR using pAG32 as a template to insert hygromycin-resistant gene (*hyg*^r) within downstream of each coding region (27). The genomic fragments containing the *ura4*⁺ or *hyg*^r reporter gene were then PCR-amplified using *Taq* polymerase (Toyobo) to introduce random mutations, and the PCR products were introduced into *S. pombe* cells to replace the

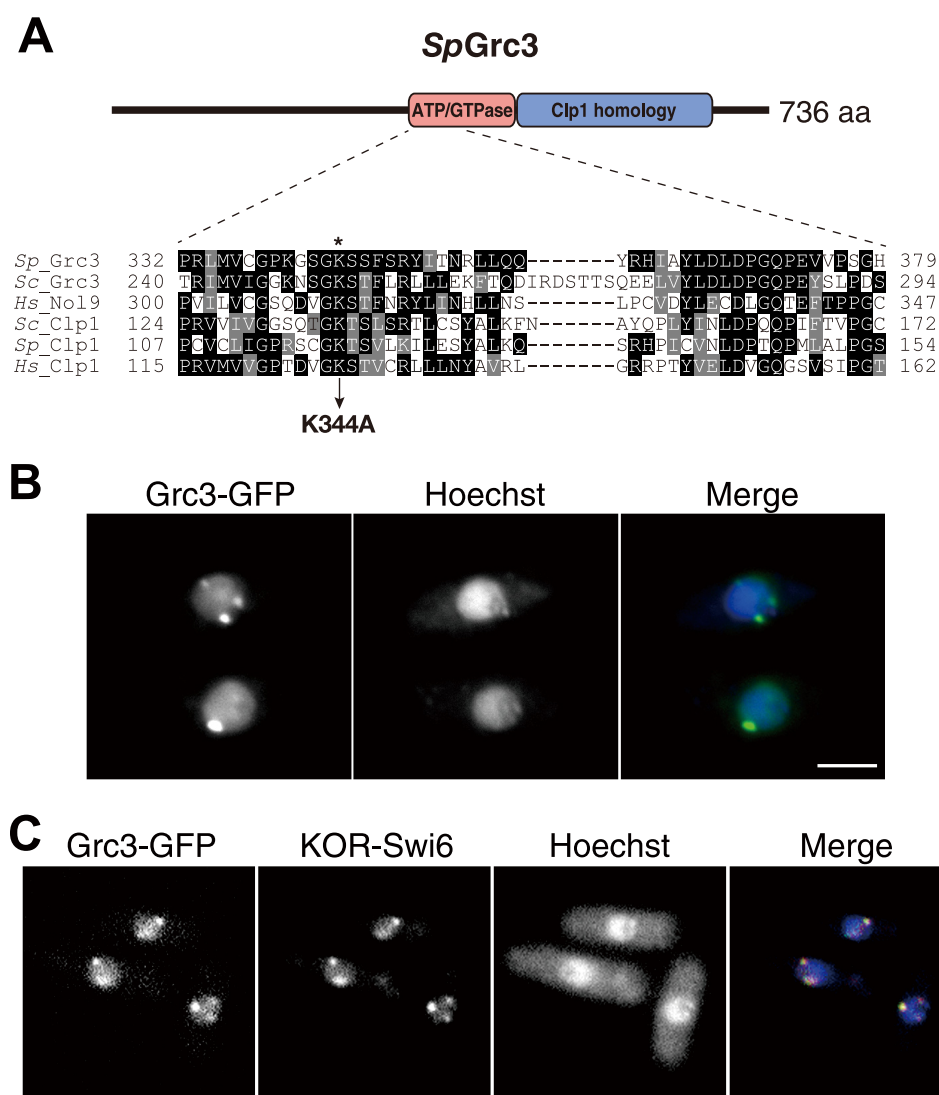


FIGURE 1. Grc3 associates with both heterochromatic and perinucleolar regions. *A*, schematic diagram of *S. pombe* Grc3. The conserved ATP/GTPase domain and Clp1 homologous region are shown (top). We used the ClustalW program to align the amino acid (aa) sequences of the conserved ATP/GTPase domain from *S. pombe* Grc3 (Sp_Grc3) and Clp1 (Sp_Clp1, product of SPAC22H10.05c); *S. cerevisiae* Grc3 (Sc_Grc3) and Clp1 (Sc_Clp1); and human Nol9 (Hs_Nol9) and Clp1 (Hs_Clp1) (bottom). Identical amino acids are shaded with black, and functionally conserved amino acids are shaded with gray. The position of amino acid substitution (K344A) used in this study is indicated. *B*, Grc3 was tagged with GFP at the C terminus and expressed from its native promoter. The *in vivo* location of Grc3-GFP was analyzed by fluorescence microscopy. DNA was visualized by incubation with Hoechst 33342. Bar, 3 μ m. *C*, co-localization of Grc3 and Swi6. Cells expressing both Grc3-GFP and Kusabira orange (KOR)-fused Swi6 were analyzed by fluorescence microscopy. Three-dimensional optical section images were taken, and the acquired images were deconvoluted. A merged image of Grc3-GFP (green), KOR-Swi6 (red), and DNA (blue) is shown at right.

wild-type allele with the mutant allele. Transformed cells were first isolated on minimal medium lacking uracil (for *grc3^{ts}*) or on YEA medium (0.5% yeast extract, 3% glucose, 75 μ g/ml adenine) containing hygromycin (for *crb3^{ts}*, *ipi1^{ts}*, *las1^{ts}*, or *rix1^{ts}*) at 25 $^{\circ}$ C, and roughly 2,000 colonies were picked up and tested for temperature-sensitive growth on a nonselective plate at 36 $^{\circ}$ C. Mutant clones showing temperature-sensitive growth were isolated and used for further analysis. The position of altered amino acids in the isolated temperature-sensitive mutants are listed in supplemental Table S3.

RNA Extraction and Northern Blot Analysis—Total RNA was extracted from cells as described previously (6). Purified total RNA samples were separated by electrophoresis on a 1.25% agarose gel containing 6.7% formaldehyde, blotted on nylon membranes, cross-linked, and hybridized with each oligonucleotide probe.

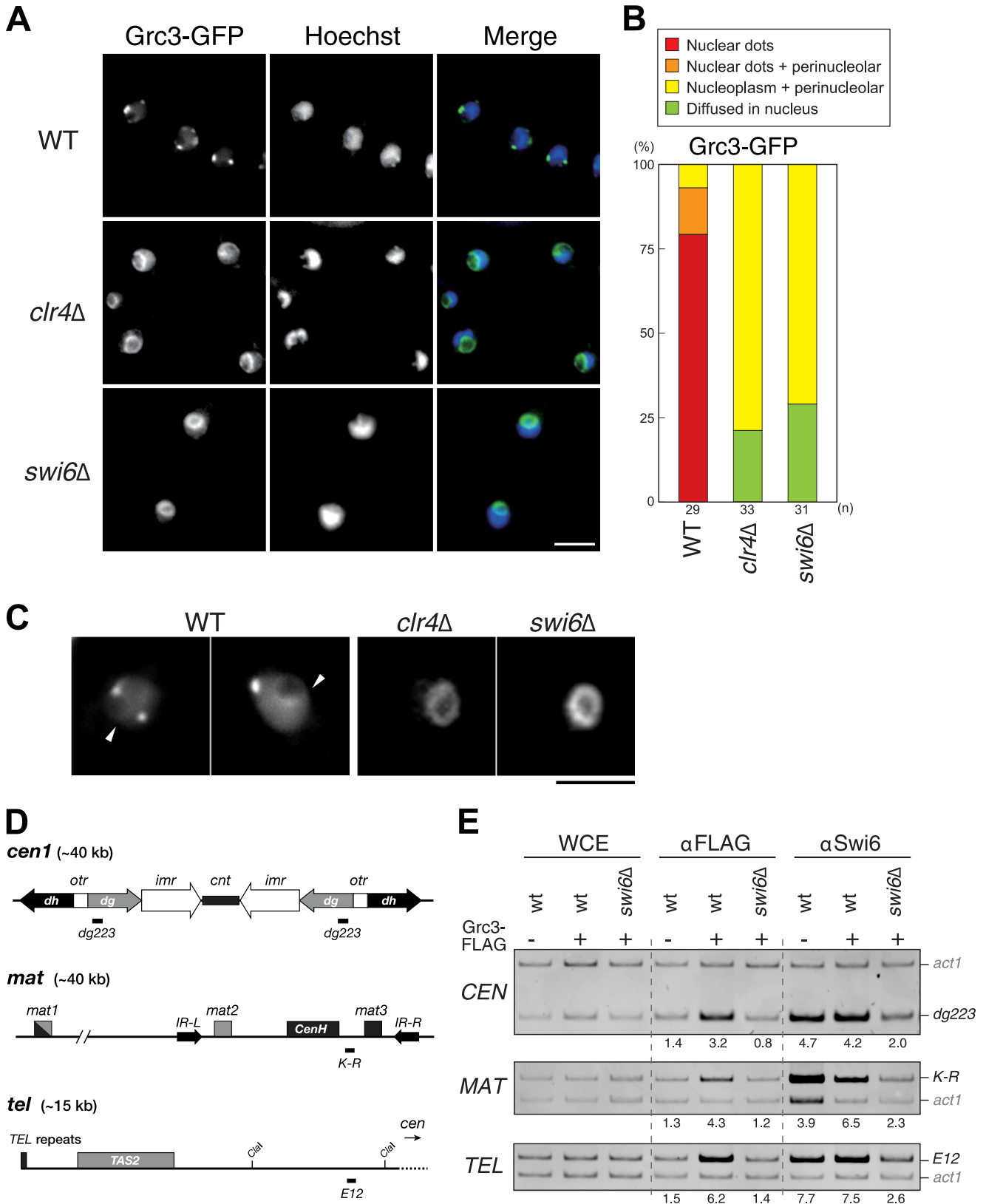
The oligonucleotides used are listed in supplemental Table S2. In time course experiments, wild-type and temperature-sensitive mutant *S. pombe* cells were first cultured at the permissive temperature (25 $^{\circ}$ C) and then shifted to the restrictive temperature (36 $^{\circ}$ C). Total RNA was prepared from cell samples obtained at each time point after temperature shifting and subjected to Northern analysis.

Multicopy Suppressor Screening—The *S. pombe* genomic library (pTN-L1; National Bio Resource Project) was introduced into the *grc3* mutant cells (SPM1617, SPM1620, or SPM1623) by electroporation. The transformed cells were incubated on a selected medium (AA-Leu) at 25 $^{\circ}$ C for 1 day and then at 34 $^{\circ}$ C for 2–10 days. Approximately 72,000 clones were screened, and 48 clones that grew at 34 $^{\circ}$ C were isolated. The plasmids were rescued in *Escherichia coli* and reintroduced

Analysis of *Grc3* Function in *S. pombe*

into *grc3* cells to confirm their ability to suppress the *grc3* mutation. The nucleotide sequences of the inserts were determined by sequencing analysis using the M13-Fw and M13-Rv primers (supplemental Table S2).

Quantitative RT-PCR Analysis—To quantify the transcribed RNAs, the total RNA was extracted from yeast cells as described above and then preincubated with RNase-free DNase I (0.4 unit/mg RNA; TaKaRa) to digest the genomic



DNA. RT-PCR was performed using the One Step SYBR PrimeScript RT-PCR kit II (TaKaRa) and a 7300 real time PCR system (ABI). The primers used in this assay are listed in [supplemental Table S2](#).

RESULTS

Grc3 Associates with Heterochromatic Regions—It has been suggested that the budding yeast Grc3 is involved in rRNA processing (18). A homologous protein of Grc3 in *S. pombe* encoded by *SPCC830.03* (hereafter referred to as *SpGrc3* or Grc3) (Fig. 1A) was identified as a factor displaying nuclear dot localization (23–25), a pattern reminiscent of heterochromatin proteins (6). To gain insight into the function of *S. pombe* Grc3, we first examined its subcellular localization by expressing C-terminally GFP-fused Grc3 (Grc3-GFP) from its native promoter. As reported in previous studies (23–25), Grc3-GFP preferentially localized to the nucleus and formed two to three discrete spots in interphase cells (Fig. 1B).

In fission yeast, three heterochromatic regions—centromeres, the mating type region, and telomeres—are visualized by immunostaining for Swi6 or GFP-fused Swi6 (6, 26). Two to five discrete Swi6 foci in interphase cells represent one large cluster entirely composed of centromeres, several clusters of telomeres, and the mating type region (26). To determine whether the dot-like localization of Grc3-GFP corresponds to heterochromatic regions, we constructed strains expressing both Grc3-GFP and N-terminally Kusabira-orange-fused Swi6 (KOR-Swi6) and compared their localization in each cell. Using a fluorescence microscope equipped with a three-dimensional deconvolution system, we confirmed that the Grc3-GFP dots clearly co-localized with the signals for KOR-Swi6 (Fig. 1C). These results suggested that *S. pombe* Grc3 localizes to the heterochromatin regions.

Heterochromatic Localization of Grc3 Is Dependent on Swi6 and Clr4—Heterochromatin assembly in fission yeast involves H3K9me, mediated by the conserved methyltransferase Clr4^{SUV39H}. H3K9me creates binding sites for Swi6^{HP1} (7). To analyze the relationship between Grc3 and heterochromatin, we examined the Grc3-GFP localization in *swi6*-deleted (*swi6*Δ) or *clr4*-deleted (*clr4*Δ) cells. Strikingly, the Grc3-GFP dot-like localization was completely abolished in these mutant cells (Fig. 2A). Furthermore, the delocalized Grc3-GFP in *swi6*Δ or *clr4*Δ cells preferentially accumulated in perinucleolar regions (Fig. 2, A and B). Careful examination of microscopic images of wild-type cells revealed that, in addition to the dot-like localization, some of the Grc3-GFP was also present in the perinucleolar region (Fig. 2C, indicated by *white arrowheads*). These results confirmed that Grc3 localizes to two nuclear domains, the heterochromatin and perinucleolar

regions, and further indicated that the Grc3 heterochromatic localization requires an intact heterochromatin structure.

The involvement of Grc3 with rRNA processing was suggested in budding yeast. However, almost nothing is known about the functional involvement of Grc3 with heterochromatin. To examine the association of Grc3 with heterochromatin directly, we performed a ChIP assay. We constructed strains expressing C-terminally 5FLAG-tagged Grc3 (Grc3-FLAG), and its association with the three heterochromatic regions, centromeres (*dg223*), the mating type region (*K-R*), and telomeres (*E12*), was determined using the *act1* locus as a negative control (Fig. 2D) (6). Consistent with our cytological analyses, Grc3-FLAG associated with the three heterochromatic regions, and importantly, this association was eliminated in the Δ*swi6* or Δ*clr4* mutant cells (Fig. 2E and data not shown). Together with the cytological analyses, these results indicated that *SpGrc3* associates with two distinct nuclear domains, the heterochromatin and perinucleolar regions, and that its heterochromatic association is dependent on Swi6 and Clr4.

Grc3 Is Required for Pre-rRNA Processing—In *S. cerevisiae*, Grc3 is essential for growth and is involved in ribosomal RNA processing (18, 22). Although a genome-wide deletion analysis revealed that fission yeast Grc3 is essential for cell viability (30), its physiological role and functional involvement in rRNA processing or heterochromatin assembly have not been explored. We replaced an allele for *grc3*⁺ in diploid cells with a hygromycin resistance gene (*hyg*^r) and confirmed that haploid cells harboring the *hyg*^r gene were not viable (Fig. 3A).

To examine the cellular function of Grc3, we replaced the original *grc3*⁺ allele with a randomly mutagenized *grc3* allele and isolated 12 temperature-sensitive (*ts*) *grc3* alleles (Fig. 3B and data not shown) (see also “Experimental Procedures” and [supplemental Table S3](#)). Using these *grc3-ts* mutant strains, we tested whether Grc3 is required for rRNA processing. Wild type and *grc3-7*, one of the *grc3-ts* mutant strains, were first cultured at the permissive temperature (25 °C) and then shifted to the nonpermissive temperature (36 °C). The total RNAs were extracted from the cells at different time points after the temperature shift and were subjected to Northern hybridization using specific oligonucleotide probes (Fig. 3C). Although no obvious growth defect was observed in the *grc3-7* mutant cells at 25 °C (Fig. 3B, *section 7*), high levels of rRNA precursors (35 and 27 S) were detected in this mutant even at the permissive temperature (Fig. 3D, *grc3-7, 0 h*). After the temperature shift, the high levels of these rRNA precursors became much more pronounced, whereas the mature 25 and 5.8 S rRNAs decreased (Fig. 3D, *grc3-7, 1–6 h*). Notably, the level of mature 18 S rRNA was not affected in the *grc3-7* mutant cells, suggesting that the

FIGURE 2. **The localization of Grc3 to the heterochromatic regions depends on Swi6 and Clr4.** A, the location of Grc3-GFP in WT, *clr4*Δ, or *swi6*Δ cells, analyzed as in Fig. 1B. Bar, 5 μm. B, the percentage of cells showing the distinct localization patterns for Grc3-GFP. C, a representative image of nucleolar localized Grc3-GFP. The *white arrow* indicates Grc3-GFP signal at the nucleolar peripheral region in wild-type cells. Bar, 2.5 μm. D, a diagram of *S. pombe* centromere 1 (*cen*), the mating type (*mat*) loci, and subtelomere (*tel*). The positions of amplified regions in the ChIP assay are indicated beneath each drawing. E, Grc3 association with the three heterochromatic regions was analyzed by ChIP assay. DNA isolated from anti-FLAG-immunoprecipitated chromatin (αFLAG) or whole cell extract (WCE) was used as a template for PCR amplifying *CEN-dg223* (224 bp), *MAT-K-R* (524 bp), or *TEL-E12* (521 bp) with *act1* (425 bp). The samples were prepared from either wild-type or *swi6*Δ cells expressing FLAG-tagged Grc3. Wild-type cells without Grc3 tagging were used as a control. Swi6 association with the indicated heterochromatic regions was assayed by ChIP using an anti-Swi6 antibody (αSwi6). The ratio of the *CEN-dg223*, *MAT-K-R*, or *TEL-E12* signals to that of *act1* in the ChIP results was calculated, and the relative fold enrichment is shown beneath each lane.

Analysis of *Grc3* Function in *S. pombe*

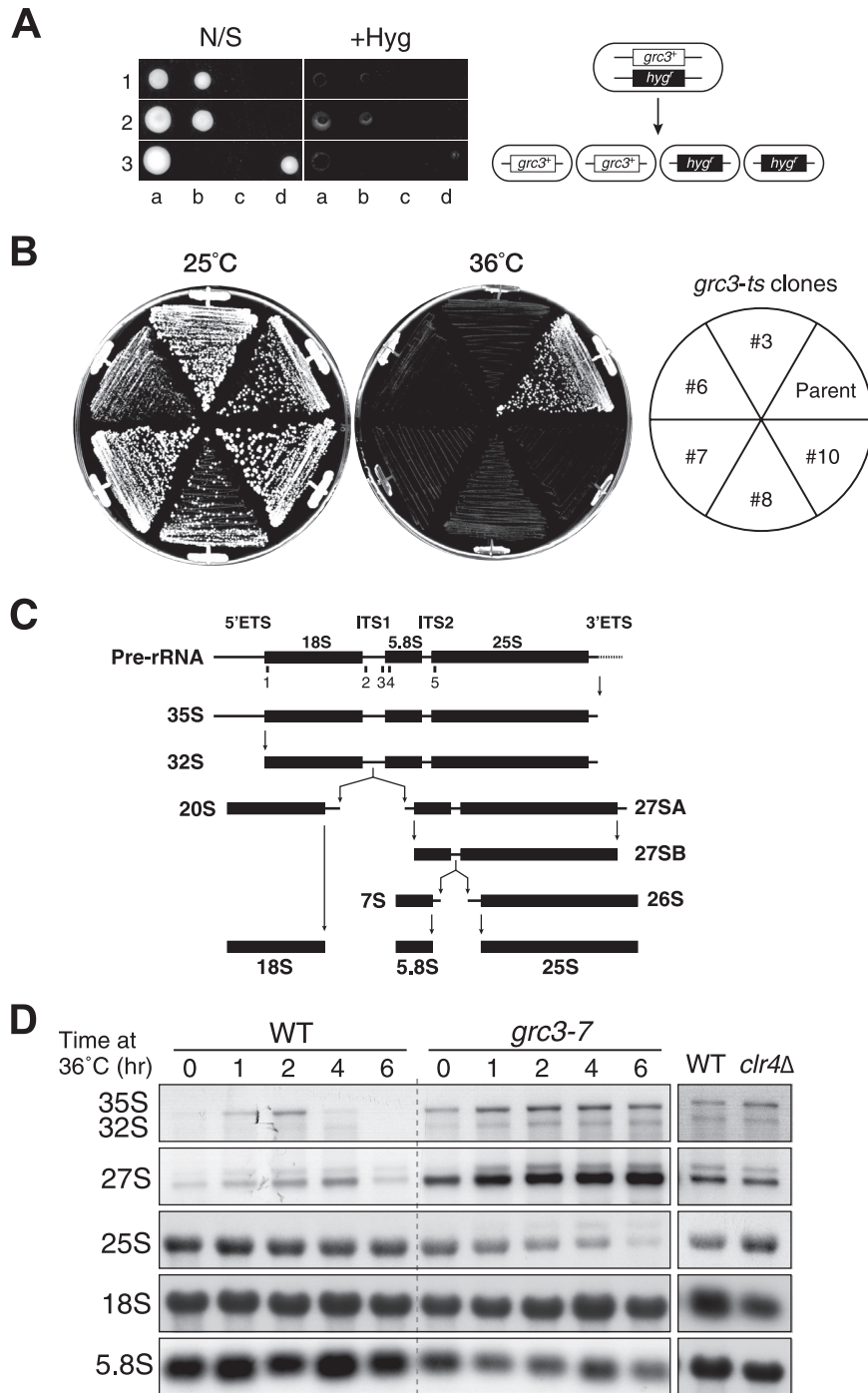


FIGURE 3. *Grc3* is required for proper ribosomal RNA processing. *A*, *Grc3* is essential for cell growth. One *grc3*⁺ allele of a diploid cell was replaced with a hygromycin resistance gene (*hyg*⁺). After sporulation, each spore was grown on nonselective (*N/S*) medium, and viable colonies were replicated on YEA medium containing hygromycin (+*Hyg*). All of the viable cells did not harbor the *grc3*::*hyg*⁺ allele. A diagram of the tetrad analysis is shown at *right*. *B*, temperature-sensitive growth of isolated *grc3* mutants. Parental wild-type (SPM1467) and *grc3* mutant (*grc3-3*, *grc3-6*, *grc3-7*, *grc3-8*, or *grc3-10*) cells were grown on YEA plates at 25 or 36 °C for 3–5 days. *C*, the ribosomal RNA processing pathways and location of oligonucleotide probes used for Northern hybridization. *Section 1*, rRNA_18S; *section 2*, NB629_2; *section 3*, NB1102_2; *section 4*, rRNA_5.8S; *section 5*, rRNA_25S. The processing pathway determined from *S. cerevisiae* studies is presented; major processing events are thought to be conserved in *S. pombe*. The transcribed spacer regions are indicated as *narrow lines*, and mature rRNA is indicated as *black rectangles*. *D*, Northern hybridization analyses of rRNAs. Wild-type and *grc3-3* cells were cultured at a permissive temperature (25 °C) in YEA medium, and then the culture was shifted to a nonpermissive temperature (36 °C). RNA was isolated from cultures at different time points and subjected to Northern hybridization analysis. rRNAs prepared from exponentially growing wild-type and *clr4Δ* cells were also analyzed.

ITS1 processing was not affected in this mutant. Similar rRNA processing defects were observed in other *grc3* mutant cells (data not shown). Together, these results indicated that *S. pombe Grc3* is required for pre-rRNA processing, especially

ITS2 processing, which is quite consistent with the results for *S. cerevisiae Grc3* (18).

***Grc3* Regulates Heterochromatin Silencing**—Our cytological analyses revealed that the majority of *Grc3* localized to hetero-

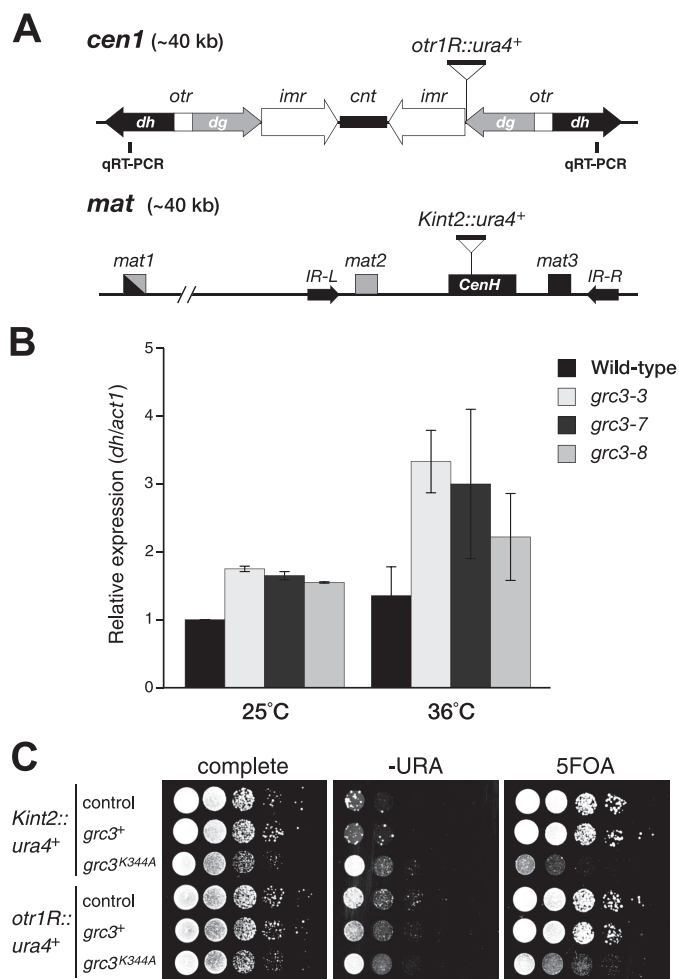


FIGURE 4. Grc3 is required for heterochromatic gene silencing. A, a diagram of *S. pombe* centromere 1 (*cen1*) and the mating type (*mat*) loci. The positions of silencing reporter genes (*otr1R::ura4+* and *Kint2::ura4+*) are shown. The target region for quantitative RT-PCR is indicated beneath the diagram of centromere 1. B, quantitative RT-PCR analysis of *cen* (*dh*) transcript levels relative to the control transcript *act1*⁺. Wild-type and *grc3* mutant cells were cultured at either the permissive (25 °C) or nonpermissive (36 °C) temperature for 20–22 h, and then the *cen* (*dh*) transcript levels were assayed and normalized to the wild type. C, *grc3*⁺ or *grc3-K344A* was overexpressed from the *nmt1* promoter of multicopy plasmids (pREP1). The empty plasmid was used as a control. A 10-fold serially diluted culture of cells harboring the indicated plasmid was spotted onto nonselective medium (complete), –Ura medium, or medium containing 5-fluoroorotic acid (5FOA).

chromatic regions, whereas only a minor fraction was associated with perinucleolar regions (Figs. 1B and 2, B and C). To examine whether Grc3 is functionally involved in heterochromatic gene silencing or heterochromatin assembly, we first tested the effect of the *grc3-ts* allele to silence a marker gene inserted in the heterochromatic regions (Fig. 4A). However, the impaired growth of the *grc3-ts* mutant cells hampered the evaluation by spotting assay (data not shown). Therefore, we assessed the function of Grc3 in heterochromatic silencing by monitoring pericentromeric *dh* transcripts (Fig. 4B).

In wild-type cells, pericentromeric transcripts are quickly processed by RNAi and/or RNA degradation pathways (13), and low levels of *dh* transcripts were detected by RT-PCR analysis (31). In *grc3* mutant cells, pericentromeric transcript levels were clearly higher than that of wild-type cells even at the permissive temperature (25 °C) (Fig. 4B, left columns). Notably, the

transcript levels were elevated at the restrictive temperature (36 °C) (Fig. 4B, right columns). These data suggest that Grc3 is involved in heterochromatin assembly in fission yeast.

Grc3 possesses a conserved ATP/GTPase motif and shows amino acid sequence similarity to Clp1, which is a component of the mRNA cleavage and polyadenylation machinery (Fig. 1A) (20, 21). Human Clp1 has been identified as an RNA kinase that phosphorylates the 5'-end of synthetic siRNAs and tRNA 3'-exons (32). A recent study showed that *S. cerevisiae* Grc3 has a similar kinase activity (33). Although we have not so far succeeded in detecting a similar kinase activity for *S. pombe* Grc3 (data not shown), it was conceivable that the ATP/GTPase domain plays a critical role in *SpGrc3* function. We introduced an Ala substitution in the ATP/GTPase domain of Grc3 (K344A; Fig. 1A), constructed plasmids to express wild type or mutant Grc3^{K344A} under the *nmt1* promoter, and examined its effect on heterochromatin silencing (Fig. 4C).

Wild-type Grc3 expression had only a minor effect on silencing at centromere 1 (*otr1R::ura4+*) or the mating type region (*Kint2::ura4+*). However, mutant Grc3^{K344A} expression impaired heterochromatin silencing, which was apparent from its robust growth on a medium lacking uracil and its increased sensitivity to 5-fluoroorotic acid (5FOA) (Fig. 4C). Mutant Grc3^{K344A} may have a dominant-negative role for proper Grc3 function in heterochromatin silencing. Together, these results demonstrated that Grc3 regulates heterochromatic silencing in fission yeast and that its ATP/GTPase domain is critical to its function.

Grc3 Interacts with Las1 and the IPI Complex—To gain further insight into the physiological function of *S. pombe* Grc3, we purified and analyzed Grc3-interacting proteins. We constructed a strain in which a functionally C-terminally TAP-tagged Grc3 protein was expressed from its endogenous promoter and purified this protein using a tandem affinity purification technique (28). Polyacrylamide gel electrophoresis and LC-MS/MS analyses revealed that Grc3 interacted with three proteins: Crb3, a WD-repeat protein encoded by *SPAC13G7.08c*; and two proteins homologous to *S. cerevisiae*, Las1 and Rix1 (encoded by *SPBC16C6.12c* and *SPCC4G3.18*, respectively) (Fig. 5, A and C). Although the functional relationships with the *S. cerevisiae* counterparts need to be cleared, we hereafter refer to these proteins as *SpLas1* and *SpRix1*, respectively.

In fission yeast, Crb3 has been shown to interact with Cut5 (34) and to assist in maintaining DNA damage checkpoints (35). On the other hand, its *S. cerevisiae* counterpart, Ipi3, joins with Ipi1 and Rix1/Ipi2 to form the protein complex IPI (involved in processing of ITS2), and all three components are required for proper ITS2 processing in pre-rRNA maturation (18, 19, 36). *S. cerevisiae* Las1 was originally characterized as an essential protein for cell viability and cell proliferation (37), and a recent report showed that the human nucleolar protein Las1 (Las1L) is essential for cell proliferation and ribosome synthesis (38). Based on sequence similarities, the fission yeast homologues are hypothesized to have a role in rRNA processing, but their physiological function is unknown.

To confirm the physical interaction among these proteins, we constructed strains expressing functional C-terminally

Analysis of *Grc3* Function in *S. pombe*

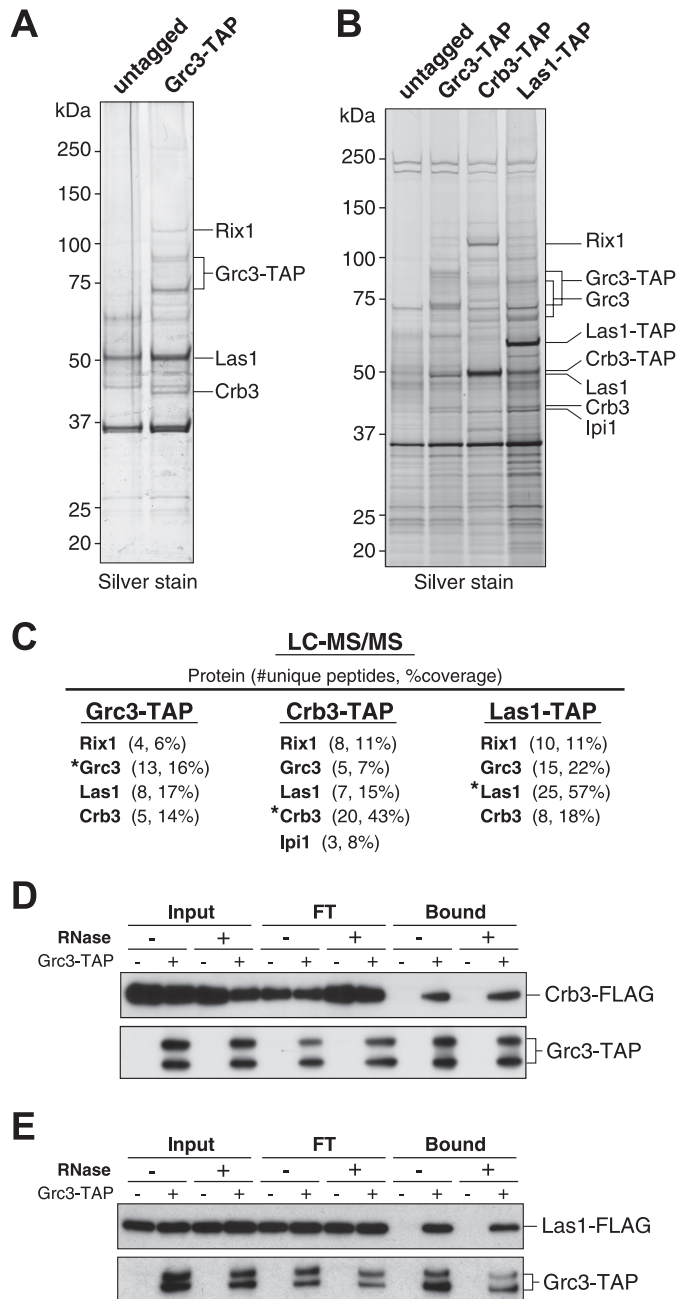


FIGURE 5. Purification of Grc3-interacting proteins, and identification of Las1 and IPI complex components. *A* and *B*, silver-stained gels show the purification of Grc3-TAP, Crb3-TAP, Las1-TAP, and an untagged control strain. The approximate position of Grc3, Las1, and IPI complex components, identified by mass spectrometry, is indicated. *C*, results of LC-MS/MS of purified proteins that interacted with Grc3-TAP, Crb3-TAP, and LAS1-TAP. Tagged proteins are indicated by asterisks. *D* and *E*, Protein extracts prepared from cells expressing both Crb3-FLAG and Grc3-TAP (*D*) or Las1-FLAG and Grc3-TAP (*E*) were subjected to immunoprecipitation using IgG-Sepharose, and bound proteins were detected by Western analysis using an anti-FLAG antibody or peroxidase anti-peroxidase complex (PAP antibody). Grc3-untagged strains were used as controls. Prior to incubation with the IgG-Sepharose, the protein extracts were mock (–) or RNaseA-treated (100 μ g of RNaseA/ml lysate) to test for the potential involvement of RNA in their interactions (see supplemental Fig. S1).

TAP-tagged Crb3 or Las1, performed tandem affinity purification, and analyzed Crb3- and Las1-interacting proteins by LC-MS/MS (Fig. 5, *B* and *C*). The results from these independent TAP purifications confirmed the interactions among Grc3,

A Suppressors of *grc3-3*

Fragment#	gene(s)	frequency
1	<i>grc3</i> ⁺	8
2	<i>las1</i> ⁺ , <i>rpl3201</i> ⁺	18
3	<i>hta1</i> ⁺ , <i>htb1</i> ⁺ , <i>sec5</i> ⁺	1
4	<i>cdc3</i> ⁺ , <i>tif33</i> ⁺	2
5	<i>rad50</i> ⁺	1
6	<i>csx1</i> ⁺	3
7	<i>duo1</i> ⁺ , <i>SPBC32F12.07c</i>	1
8	<i>cpc2</i> ⁺	1
total		35

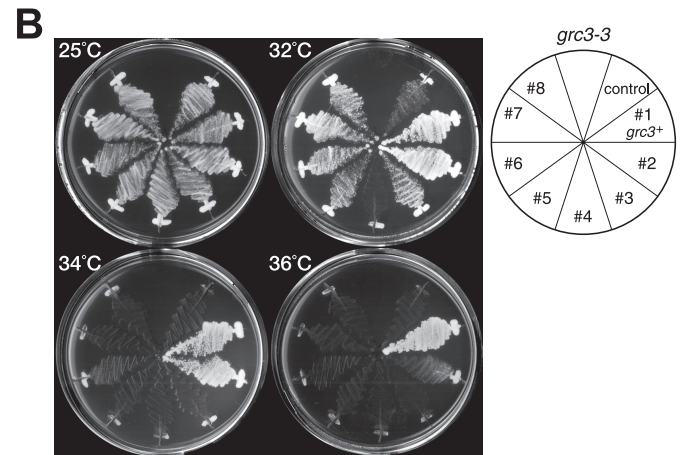
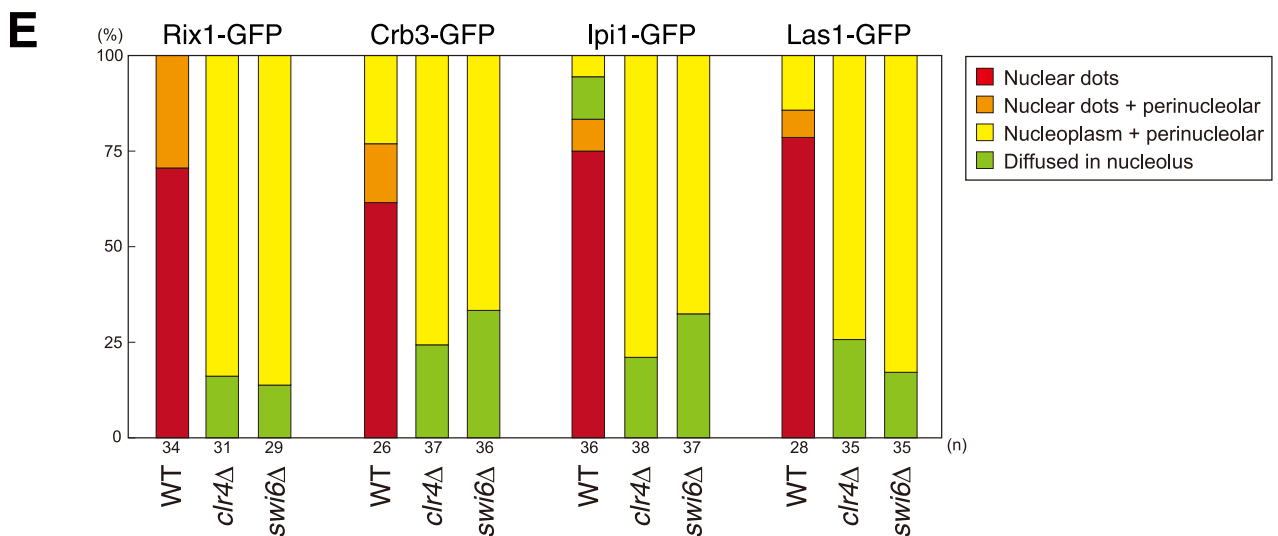
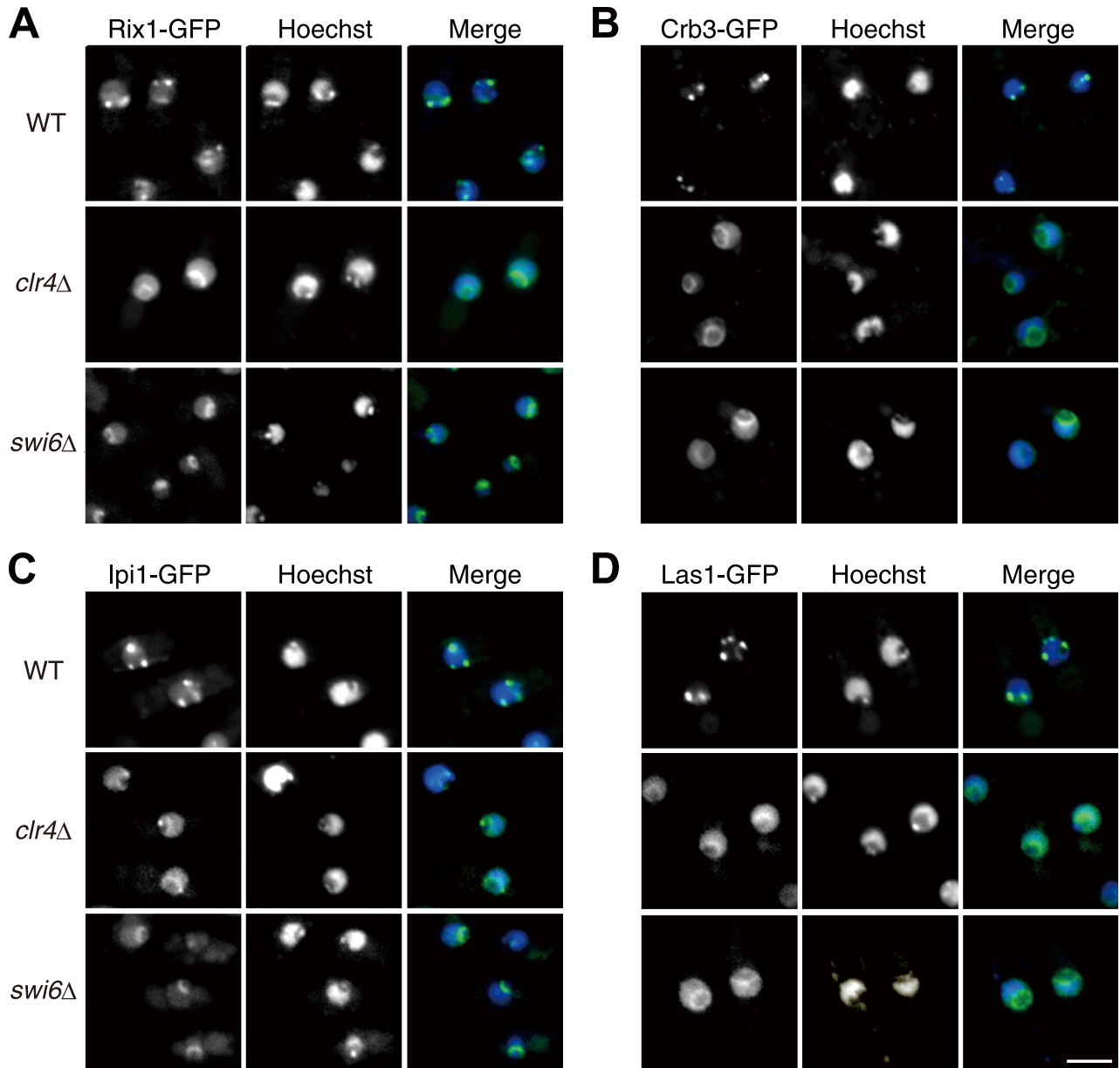


FIGURE 6. Identification of *las1*⁺ as a multicopy suppressor of the *grc3* mutant. *A*, a summary of multicopy suppressors identified for the *grc3-3* mutant. *B*, the *grc3-3* mutant (SPM1617) harboring a control plasmid or each of the isolated genomic fragments (sections 1–8) was streaked onto –Leu plates and incubated at 25, 32, 34, or 36 °C for 2–5 days. *C*, *las1*⁺ alleviates the *grc3-3* temperature sensitivity. A *grc3-3* mutant harboring a control pREP1 or pREP1-*las1*⁺ was spotted onto a –Leu plate and incubated at 25, 32, or 34 °C for 5–8 days.

Rix1, Crb3, and Las1. Although we failed to detect a fission yeast homologue of Ipi1 (encoded by *SPCC1393.06c*) in the initial Grc3-TAP purification (Fig. 5*A*), it was detected in the Crb3-TAP purification (Fig. 5*C*), thus suggesting that Ipi1, Rix1, and Crb3 form a similar IPI complex in fission yeast and that this IPI complex is functionally linked with Grc3 and Las1.

To rule out the possibility that these proteins interact indirectly via cellular RNAs, we constructed strains expressing Grc3-TAP in conjunction with Crb3-FLAG or Las1-FLAG and conducted pull-down experiments with or without RNase treatment (Fig. 5, *D* and *E*, and supplemental Fig. S1). In agreement with the TAP purification, Crb3-FLAG and Las1-FLAG were efficiently co-immunoprecipitated with Grc3-TAP, and these interactions were resistant to RNase treatment (Fig. 5, *D* and *E*). We therefore conclude that Grc3 stably interacts with both IPI complex and Las1, in an RNA-independent manner.



Analysis of Grc3 Function in *S. pombe*

Identification of *las1*⁺ as a Multicopy Suppressor of *grc3* Mutation—To search for factors that genetically interact with *grc3*⁺, we screened for multicopy suppressors of the *grc3* mutation. The genomic library of *S. pombe* was introduced into the *grc3-3*, *grc3-7*, or *grc3-8* mutant, and viable cells were selected at a nonpermissive temperature (34 °C). Among the 1–2 × 10⁵ clones screened, we obtained a total of 48 clones as candidate genes to suppress temperature sensitivity in *grc3* mutations. Nucleotide sequencing of the harbored plasmids revealed that 21 clones turned out to contain *grc3*⁺ genomic DNA (data not shown). Whereas only *grc3*⁺-containing plasmid was identified for screening using *grc3-7* or *grc3-8*, a number of additional genomic fragments were isolated as suppressors for *grc3-3* (Fig. 6A). Notably, the most abundant genomic clones were genomic DNA containing *las1*⁺. Although several other genomic fragments were isolated as suppressors of the *grc3-3* temperature-sensitive phenotype (Fig. 6A), their suppressive effect was much weaker than that of the plasmid containing *las1*⁺ (Fig. 6B, compare section 2 with other plasmids). It is thus likely that the harbored gene(s) indirectly affected the temperature sensitivity of the *grc3-3* mutant cells.

To confirm the suppressive effect of *las1*⁺, we introduced a *las1*⁺-containing plasmid (pREP1-*las1*⁺) into the *grc3-3* cells. The temperature sensitivity was indeed relieved at 32 °C, although the temperature-sensitive growth was not clearly reversed at 34 °C (Fig. 6C). These data indicate that Las1 can suppress the temperature sensitivity of *grc3-3* and further strengthened a functional link between Grc3 and Las1. Because the *las1*⁺-containing plasmid only weakly suppressed the *grc3-7* and *grc3-8* (data not shown), the *grc3-3* allele may have a specific mutation(s) in the region responsible for binding to Las1.

***Las1* and IPI Complex Components Localize to Heterochromatic Regions**—To examine functional correlations between Grc3-interacting proteins, we examined the subcellular localizations of Crb3, Rix1, Ipi1, and Las1 by expressing C-terminally GFP-fused proteins from their endogenous promoters. Although the subcellular localization of some of these Grc3-interacting proteins has been described previously (24, 25), we confirmed that all of these proteins preferentially localized to the nucleus and formed nuclear spots (Fig. 7). As observed for Grc3-GFP, these nuclear spots were clearly co-localized with the signals for KOR-Swi6 (supplemental Fig. S2). Importantly, deleting *swi6* or *clr4* caused these nuclear spots to delocalize and led to a characteristic localization pattern surrounding the nucleolus (Fig. 7, A–D, *clr4*Δ and *swi6*Δ). Quantification of the subcellular localization further confirmed a close link between Grc3 and its interacting proteins (compare Fig. 7E with Fig. 2B). These results suggested that Las1 and the IPI complex components also associate with the heterochromatic regions and that they are functionally correlated with Grc3.

Grc3-interacting Proteins Are Required for Both Pre-rRNA Processing and Heterochromatic Gene Silencing—Although functional involvement of IPI complex components in rRNA processing had been described previously in *S. cerevisiae* (18, 19), the physiological roles of IPI complex components and Las1 in fission yeast have yet to be determined. We first confirmed that these proteins are essential for cell viability (data not shown) (30). To further investigate their cellular function, we isolated temperature-sensitive mutant alleles for *crb3*⁺, *ipi1*⁺, *las1*⁺, or *rix1*⁺ by PCR-based mutagenesis method (see “Experimental Procedures” and supplemental Fig. S3 and supplemental Table S3) and tested whether these factors are required for rRNA processing. We found that the temperature-sensitive mutants *crb3-3*, *ipi1-1*, *las1-1*, or *rix1-2* accumulated rRNA precursors (35 and 27 S) at the nonpermissive temperature (Fig. 8A). Similar rRNA processing defects were observed in other mutant cells (data not shown).

We next tested whether Grc3-interacting proteins were also required for heterochromatic silencing. We found that higher levels of pericentromeric transcripts were accumulated in *crb3-3*, *las1-1*, or *rix1-2* mutant cells at the nonpermissive temperature when compared with wild-type cells (Fig. 8B). The effect of *ipi1-1* was weaker than that of other conditional mutants. Ipi1 may have distinct function in heterochromatic silencing. Together, these results suggest that Grc3-interacting proteins are also required for both rRNA processing and heterochromatin assembly in fission yeast.

DISCUSSION

In this report, we demonstrated that the fission yeast Grc3 localizes to both heterochromatin and perinucleolar regions and has a dual role in rRNA processing and heterochromatin silencing. Our biochemical and cytological analyses further revealed that Grc3 is functionally linked with Las1 and the IPI complex. Our findings suggest that rRNA processing and heterochromatic silencing use a shared molecular mechanism that involves Grc3 and its interacting partners.

Previous studies have shown that *S. cerevisiae* Grc3 is required for ITS2 processing in 27 S pre-rRNA maturation. Using temperature-sensitive mutant cells, we confirmed that *S. pombe* Grc3 also plays a role in this particular step of rRNA processing. We observed an accumulation of 27 S pre-rRNA and decreased levels of mature 5.8 and 25 S rRNAs in *grc3* mutant cells (Fig. 3D). Because the human homologue Nol9 was identified as a nucleolar protein (39), it is conceivable that the Grc3 homologous protein has a conserved role in rRNA processing. Several observations supported the direct involvement of Grc3 in rRNA processing. Grc3 was observed, together with ribosomal proteins, in a protein fraction that was isolated by Rai1 affinity purification (40). In addition, *grc3* mutation did not affect the amount of small nucleolar RNAs involved in

FIGURE 7. **Las1 and IPI complex component localization to heterochromatic regions is dependent on Swi6 and Clr4.** A–D, the Grc3-interacting proteins Rix1, Crb3, Ipi1, and Las1 were tagged with GFP at the C terminus and expressed from their native promoter. The *in vivo* locations of Rix1-GFP (A), Crb3-GFP (B), Ipi1-GFP (C), and Las1-GFP (D) in WT, *clr4*Δ, or *swi6*Δ cells were analyzed by fluorescence microscopy. DNA was visualized by Hoechst 33342. Co-localization of each GFP fusion protein with KOR-Swi6 is shown in supplemental Fig. S2. Bar, 5 μm. E, the percentage of cells showing the distinct localization patterns for Rix1-GFP, Crb3-GFP, Ipi1-GFP, or Las1-GFP.

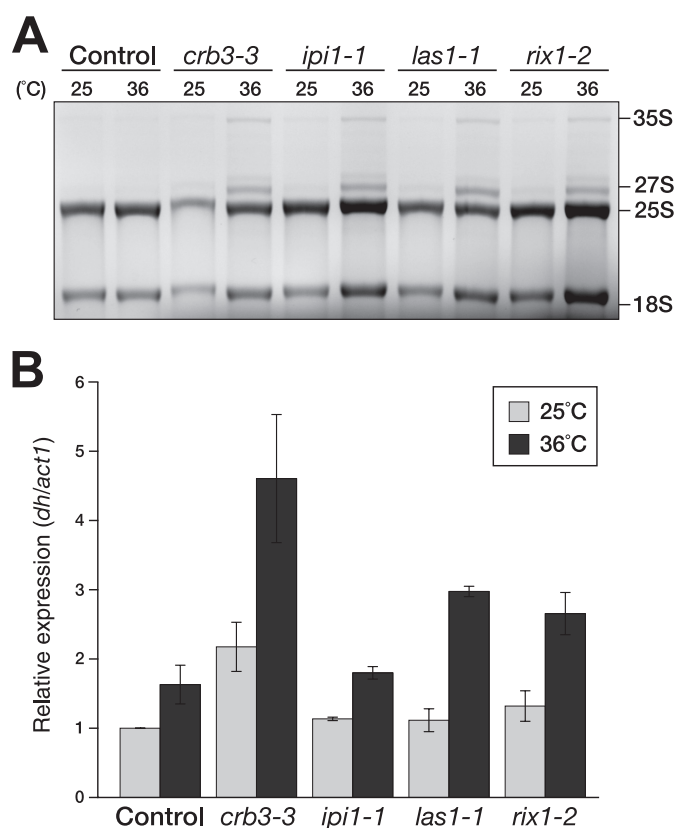


FIGURE 8. Las1 and IPI complex components are required for both ribosomal RNA processing and heterochromatin assembly. *A*, wild-type cells and temperature-sensitive mutants (*crb3-3*, *ipi1-1*, *las1-1*, and *rix1-2*) were cultured at a permissive temperature (25 °C) in YEA medium, and then the culture was shifted to a nonpermissive temperature (36 °C) for 9 h. Total RNA was isolated from cultures at permissive and nonpermissive temperatures, separated by electrophoresis on a 1.25% agarose gel, and visualized by EtBr. *B*, quantitative RT-PCR analysis of *cen* (*dh*) transcript levels relative to the control transcript *act1*⁺. Wild-type cells and temperature-sensitive mutants (*crb3-3*, *ipi1-1*, *las1-1*, and *rix1-2*) were cultured at either the permissive (25 °C) or nonpermissive (36 °C) temperature for 9 h, and then the *cen* (*dh*) transcript levels were assayed and normalized to the wild type.

rRNA processing (data not shown). Characterizing the enzymatic activity associated with Grc3 may help to explain its role in processing rRNA.

Grc3 has an amino acid sequence similarity with Clp1, a component of the mRNA cleavage and polyadenylation machinery (20, 21). Human Clp1 has been shown to have RNA kinase activity that phosphorylates the 5'-end of synthetic siRNAs and tRNA 3'-exons (32). However, no such activity has been identified for *S. cerevisiae* Clp1 (41, 42). Because the archaeal Clp1 homologue has polynucleotide kinase activity, it has been suggested that ancestral Clp1 also possesses enzymatic activity (43). A recent study showed that *S. cerevisiae* Grc3 has a similar kinase activity (33). Considering the high sequence similarity and evolutionary conservation, it is likely that *S. pombe* Grc3 has a similar kinase activity and provides phosphorylation on the cleaved RNA product for efficient degradation mediated by exonuclease(s). In this study, although we showed that the ATP/GTPase domain is critical for the function of Grc3 in heterochromatic silencing (Fig. 4C), we could not obtain direct evidence of *S. pombe* Grc3 kinase activity (data not shown). It is possible that Grc3 needs other factors or optimized assay conditions to exert its enzymatic activity or that its

ATPase activity is used in other enzymatic processes. Although a recent study showed that *S. cerevisiae* Grc3 is involved in the transcriptional termination of RNA polymerase I (33), it is not clear how a polymerase I termination defect leads to a ITS2-specific processing defect. We favor the view that Grc3 and other exonuclease activities specifically participate in ITS2 processing. The enzymatic activity of Grc3 may facilitate the efficient degradation of structured RNAs.

In this study, we showed a functional and physical link between Grc3, IPI complex components, and Las1. Although genome-wide studies on *S. cerevisiae* showed that Grc3 and IPI complex components are required for ITS2 processing, this study provides direct evidence for their functional link. A recent study showing that human Las1L functions in ribosome synthesis (38) further supports our observations. Las1 was originally identified in a genetic screening of *S. cerevisiae* mutants that could not grow in the absence of an *SSD1-v* allele (lethal in the absence of *SSD1-v*) and was shown to be an essential protein involved in cell morphogenesis and cell surface growth (37). Another recent study revealed that *Ssd1* is an RNA-binding protein that preferentially targets transcripts that encode cell wall and bud proteins (44). Although how nuclear-localized Las1 affects *Ssd1*-bound transcripts remains unclear, Las1 may modulate RNA secondary structure; using such activity, Las1 might alter *Ssd1*-bound RNAs so they can be efficiently transferred to their particular cellular compartments and similarly prepare ITS2 RNA to be efficiently processed by other factors.

We found that Grc3 and its interacting proteins localize to heterochromatin (Figs. 1 and 7) and that their heterochromatic localization is largely dependent on Swi6 and Clr4. Although heterochromatic localization does not indicate a functional involvement with heterochromatin, it is likely that their activity is linked with heterochromatin assembly. In fission yeast, heterochromatic transcripts are processed by the RNAi pathway and/or by an exosome-mediated degradation process (14, 15). Considering that ITS2 can form complex secondary structures, it is possible that Grc3 and its interacting proteins function to target transcripts with a rigid secondary structure and facilitate their degradation in combination with exonuclease activity such as Rat1. Because heterochromatin localization has not been described for *S. cerevisiae* counterparts (36), heterochromatin assembly in fission yeast, and probably other higher eukaryotes, may be coupled with active RNA degradation processes involving Grc3 activity.

Acknowledgments—We thank Y. Hiraoka, D.-Q. Ding, and K. Tatebayashi for the strains, K. Tanaka for technical advice for temperature-sensitive mutant screening, and M. Saito and F. Ishikawa for mass spectrometry analysis support. We also thank our laboratory members at the RIKEN Center for Developmental Biology for helpful discussions and S. Seno for excellent secretarial work.

REFERENCES

1. Spector, D. L. (2003) *Annu. Rev. Biochem.* **72**, 573–608
2. McStay, B., and Grummt, I. (2008) *Annu. Rev. Cell Dev. Biol.* **24**, 131–157
3. Grewal, S. I., and Moazed, D. (2003) *Science* **301**, 798–802
4. Peng, J. C., and Karpen, G. H. (2007) *Nat. Cell Biol.* **9**, 25–35
5. Bannister, A. J., Zegerman, P., Partridge, J. F., Miska, E. A., Thomas, J. O.,

Analysis of *Grc3* Function in *S. pombe*

- Allshire, R. C., and Kouzarides, T. (2001) *Nature* **410**, 120–124
6. Sadaie, M., Iida, T., Urano, T., and Nakayama, J. (2004) *EMBO J.* **23**, 3825–3835
7. Nakayama, J., Rice, J. C., Strahl, B. D., Allis, C. D., and Grewal, S. I. (2001) *Science* **292**, 110–113
8. Sadaie, M., Kawaguchi, R., Ohtani, Y., Arisaka, F., Tanaka, K., Shirahige, K., and Nakayama, J. (2008) *Mol. Cell Biol.* **28**, 6973–6988
9. Grewal, S. I., and Jia, S. (2007) *Nat. Rev.* **8**, 35–46
10. Volpe, T. A., Kidner, C., Hall, I. M., Teng, G., Grewal, S. I., and Martienssen, R. A. (2002) *Science* **297**, 1833–1837
11. Verdel, A., Jia, S., Gerber, S., Sugiyama, T., Gygi, S., Grewal, S. I., and Moazed, D. (2004) *Science* **303**, 672–676
12. Motamedi, M. R., Verdel, A., Colmenares, S. U., Gerber, S. A., Gygi, S. P., and Moazed, D. (2004) *Cell* **119**, 789–802
13. Bühler, M., and Moazed, D. (2007) *Nat. Struct. Mol. Biol.* **14**, 1041–1048
14. Bühler, M., Haas, W., Gygi, S. P., and Moazed, D. (2007) *Cell* **129**, 707–721
15. Murakami, H., Goto, D. B., Toda, T., Chen, E. S., Grewal, S. I., Martienssen, R. A., and Yanagida, M. (2007) *PLoS One.* **2**, e317
16. Venema, J., and Tollervey, D. (1999) *Annu. Rev. Genet.* **33**, 261–311
17. Tschochner, H., and Hurt, E. (2003) *Trends Cell Biol.* **13**, 255–263
18. Peng, W. T., Robinson, M. D., Mnaimneh, S., Krogan, N. J., Cagney, G., Morris, Q., Davierwala, A. P., Grigull, J., Yang, X., Zhang, W., Mitsakakis, N., Ryan, O. W., Datta, N., Jojic, V., Pal, C., Canadien, V., Richards, D., Beattie, B., Wu, L. F., Altschuler, S. J., Rowley, S., Frey, B. J., Emili, A., Greenblatt, J. F., and Hughes, T. R. (2003) *Cell* **113**, 919–933
19. Krogan, N. J., Peng, W. T., Cagney, G., Robinson, M. D., Haw, R., Zhong, G., Guo, X., Zhang, X., Canadien, V., Richards, D. P., Beattie, B. K., Lalev, A., Zhang, W., Davierwala, A. P., Mnaimneh, S., Starostine, A., Tikuisis, A. P., Grigull, J., Datta, N., Bray, J. E., Hughes, T. R., Emili, A., and Greenblatt, J. F. (2004) *Mol. Cell.* **13**, 225–239
20. Minvielle-Sebastia, L., Preker, P. J., Wiederkehr, T., Strahm, Y., and Keller, W. (1997) *Proc. Natl. Acad. Sci. U.S.A.* **94**, 7897–7902
21. de Vries, H., Rügsegger, U., Hübner, W., Friedlein, A., Langen, H., and Keller, W. (2000) *EMBO J.* **19**, 5895–5904
22. El-Moghazy, A. N., Zhang, N., Ismail, T., Wu, J., Butt, A., Ahmed Khan, S., Merlotti, C., Cara Woodwark, K., Gardner, D. C., Gaskell, S. J., and Oliver, S. G. (2000) *Yeast* **16**, 277–288
23. Ding, D. Q., Tomita, Y., Yamamoto, A., Chikashige, Y., Haraguchi, T., and Hiraoka, Y. (2000) *Genes Cells* **5**, 169–190
24. Matsuyama, A., Arai, R., Yashiroda, Y., Shirai, A., Kamata, A., Sekido, S., Kobayashi, Y., Hashimoto, A., Hamamoto, M., Hiraoka, Y., Horinouchi, S., and Yoshida, M. (2006) *Nat. Biotechnol.* **24**, 841–847
25. Hayashi, A., Ding, D. Q., Da-Qiao, D., Tsutsumi, C., Chikashige, Y., Masuda, H., Haraguchi, T., and Hiraoka, Y. (2009) *Genes Cells* **14**, 217–225
26. Ekwall, K., Javerzat, J. P., Lorentz, A., Schmidt, H., Cranston, G., and Allshire, R. (1995) *Science* **269**, 1429–1431
27. Krawchuk, M. D., and Wahls, W. P. (1999) *Yeast* **15**, 1419–1427
28. Gould, K. L., Ren, L., Feoktistova, A. S., Jennings, J. L., and Link, A. J. (2004) *Methods* **33**, 239–244
29. Sadaie, M., Shinmyozu, K., and Nakayama, J. (2008) *J. Biol. Chem.* **283**, 7185–7195
30. Kim, D. U., Hayles, J., Kim, D., Wood, V., Park, H. O., Won, M., Yoo, H. S., Duhig, T., Nam, M., Palmer, G., Han, S., Jeffery, L., Baek, S. T., Lee, H., Shim, Y. S., Lee, M., Kim, L., Heo, K. S., Noh, E. J., Lee, A. R., Jang, Y. J., Chung, K. S., Choi, S. J., Park, J. Y., Park, Y., Kim, H. M., Park, S. K., Park, H. J., Kang, E. J., Kim, H. B., Kang, H. S., Park, H. M., Kim, K., Song, K., Song, K. B., Nurse, P., and Hoe, K. L. (2010) *Nat. Biotechnol.* **28**, 617–623
31. Kato, H., Goto, D. B., Martienssen, R. A., Urano, T., Furukawa, K., and Murakami, Y. (2005) *Science* **309**, 467–469
32. Weitzer, S., and Martinez, J. (2007) *Nature* **447**, 222–226
33. Braglia, P., Heindl, K., Schleiffer, A., Martinez, J., and Proudfoot, N. J. (2010) *EMBO Rep.* **11**, 758–764
34. Saka, Y., Esashi, F., Matsusaka, T., Mochida, S., and Yanagida, M. (1997) *Genes Dev.* **11**, 3387–3400
35. Taricani, L., and Wang, T. S. (2006) *Mol. Biol. Cell.* **17**, 3456–3468
36. Galani, K., Nissan, T. A., Petfalski, E., Tollervey, D., and Hurt, E. (2004) *J. Biol. Chem.* **279**, 55411–55418
37. Doseff, A. I., and Arndt, K. T. (1995) *Genetics* **141**, 857–871
38. Castle, C. D., Cassimere, E. K., Lee, J., and Denicourt, C. (2010) *Mol. Cell Biol.* **30**, 4404–4414
39. Scherl, A., Couté, Y., Déon, C., Callé, A., Kindbeiter, K., Sanchez, J. C., Greco, A., Hochstrasser, D., and Diaz, J. J. (2002) *Mol. Biol. Cell.* **13**, 4100–4109
40. Sydorsky, Y., Dilworth, D. J., Yi, E. C., Goodlett, D. R., Wozniak, R. W., and Aitchison, J. D. (2003) *Mol. Cell Biol.* **23**, 2042–2054
41. Noble, C. G., Beuth, B., and Taylor, I. A. (2007) *Nucleic Acids Res.* **35**, 87–99
42. Ramirez, A., Shuman, S., and Schwer, B. (2008) *RNA* **14**, 1737–1745
43. Jain, R., and Shuman, S. (2009) *RNA* **15**, 923–931
44. Hogan, D. J., Riordan, D. P., Gerber, A. P., Herschlag, D., and Brown, P. O. (2008) *PLoS Biol.* **6**, 2297–2313